The Discovery of a Higgs Boson at the LHC

Bruce Mellado

University of the Witwatersrand, 1 Jan Smuts Avenue, Johannesburg 2000, South Africa

E-mail: bruce.mellado@wits.ac.za

Abstract. The Standard Model, SM, of electro-weak and strong interactions successfully describes collider data. However, weak bosons, quarks and leptons are massive. The mechanism of spontaneous electro-weak symmetry breaking is introduced in the SM in order to reconcile weak boson and fermion masses with gauge invariance of the theory. In its minimal expression this mechanism leads to a new physical state, a scalar boson, usually referred to as the Higgs boson. The ATLAS and CMS collaborations at the Large Hadron Collider have observed a new particle consistent with a scalar boson and with a mass of about 125 GeV.

1. Introduction

In the Standard Model, SM, of electro-weak, EW, and strong interactions, there are four types of gauge vector bosons (gluon, photon, W and Z) and twelve types of fermions (six quarks and six leptons) [1, 2, 3, 4]. These particles have been observed experimentally. At present, all the data obtained from the many experiments in particle physics are in agreement with the Standard Model. In the Standard Model, there is one particle, the Higgs boson, that is responsible for giving masses to all the elementary particles [5, 6, 7, 8]. In this sense, the Higgs particle occupies a unique position.

In July 2012 the ATLAS and CMS experiments reported the discovery of a boson, a Higgs-like particle with a mass $m_H \approx 125$ GeV based on the data accumulated during 2011 and part of 2012 periods [9, 10]. The Tevatron experiments have reported an excess of events consistent with this observation in the decay to bottom and anti-bottom quarks [11]. It is also relevant to note that no additional Higgs bosons with couplings as in the Standard Model have been observed in the range of $m_H < 600$ GeV.

2. Production and Decays

For the calculation of the particle production cross sections in proton-proton collision it is necessary to briefly discuss the factorization theorem. The production of particle can be viewed as the result of the scattering of partons of the incoming hadrons. It can be shown that the production cross section of a process Y, $\sigma(AB \to Y + X)$, where A and B pertain to the incoming protons and X refers to the proton remnants that do not participate in the production of process Y, can be obtained from [12, 13]:

$$\sigma(AB \to Y + X) = \sum_{a,b} \int dx_a dx_b f(x_a, \mu_F^2) f(x_b, \mu_F^2) \times \frac{d\hat{\sigma}_{ab\to Y}(x_a, x_b, \mu_R^2)}{dx_a dx_b}. \quad (1)$$

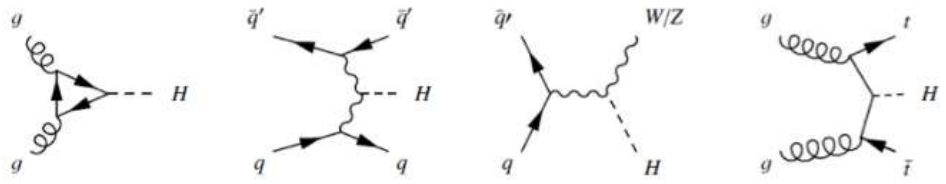

Figure 1. Leading Order Feynmann diagrams for the dominant processes involving the production of a SM Higgs boson at the LHC. From left to right: gluon-gluon fusion, Vector Boson Fusion, associated production with weak bosons and associated production with top quarks.

Table 1. Summary of QCD and EW higher order corrections currently available for the leading production mechanisms of the SM Higgs boson. Cross sections (from Ref. [14]) are given for $\sqrt{s} = 7, 8$ TeV in pb for $m_H = 125$ GeV, including the corresponding theory uncertainties.

	ggF	VBF	WH	ZH	$t\bar{t}H$
QCD	NNLO+NNLL	NNLO	NNLO		NLO
EW	NLO	NLO	NLO		LO
$\sigma(7$ TeV$)$	$15.32^{+14.7\%}_{-14.9\%}$	$1.222^{+2.8\%}_{-2.4\%}$	$0.5729^{+3.7\%}_{-4.3\%}$	$0.3158^{+4.9\%}_{-5.1\%}$	$0.0863^{+11.8\%}_{-17.8\%}$
$\sigma(8$ TeV$)$	$19.52^{+14.7\%}_{-14.7\%}$	$1.578^{+2.8\%}_{-3.0\%}$	$0.6966^{+3.7\%}_{-4.1\%}$	$0.3943^{+5.1\%}_{-5.0\%}$	$0.1302^{+11.6\%}_{-17.1\%}$

Here the subscripts a and b refer to partons (quarks and gluons) of protons A and B, respectively. Parton density functions, pdfs, are denoted with $f(x)$ where $x = x_a, x_b$ and x_a (x_b) is the fraction of the proton A (B) carried by parton a (b). At LO the proton pdfs can be interpreted as the probability of finding a parton with the fraction x of the momentum of the proton. The factorization scale, μ_F is viewed as the scale that disentangles long-distance (non-perturbative) and short-distance (perturbative) strong interactions. The pdfs are considered to be universal long-distance functions that are extracted from the data, primarily from deep inelastic scattering. The partonic cross section, $\hat{\sigma}_{ab\to Y}$, is calculable with perturbative QCD. Because the cross section is known to a finite number of orders in perturbation a residual dependence of the cross section due to the choice of scales needs to be taken into account as a theoretical uncertainty in the prediction. Scale-driven variations of the cross section are typically calculated by taking the largest variations by changing the renormalization and factorization scales by factors of two. This includes variations of both scales in the directions and all other combinations that for which the ratio of the scales is not larger than a factor of two. Uncertainties related to pdfs are also taken into account.

The Standard Model Higgs boson is produced at the LHC via several mechanisms. These are determined by the way the Higgs boson couples to SM particles. Figure 1 displays the LO Feynmann diagrams of the leading production mechanisms in proton-proton collisions. From left to right Fig. 1 displays the diagrams for gluon-gluon fusion, ggF, vector boson fusion, VBF, associated production with weak bosons and associated production with top quarks.

Figure 2 shows the production cross sections for the different Higgs boson production mechanisms, as outlined in Fig. 1. Cross sections are reported as a function of the Higgs boson mass and for the center of mass energy of $\sqrt{s} = 7$ TeV. The leading production mechanism is ggF, constituting about 90% of the total production cross section. This is to a large extent due to the large gluon flux at the LHC.

Table 1 displays the order up to which the radiative higher order EW and QCD radiative

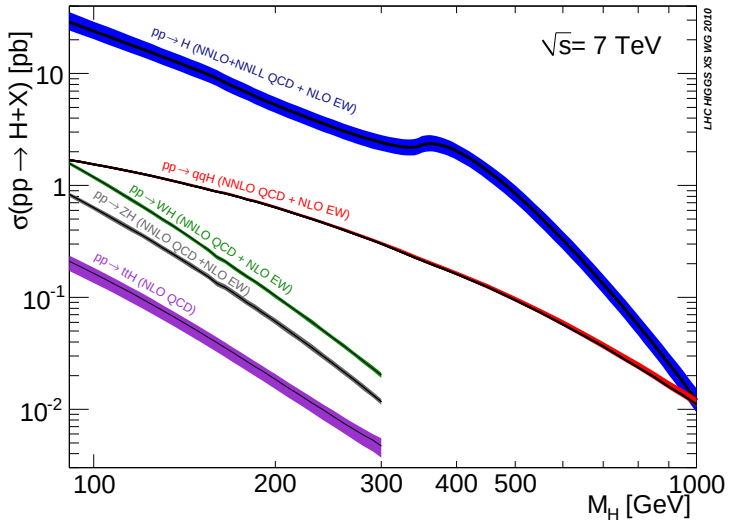

Figure 2. Standard Model Higgs boson production cross sections (in pb) for proton-proton collisions at $\sqrt{s} = 7$ TeV center of mass energy as a function of m_H (from Ref. [14]). The bands correspond to the current status of the theoretical errors.

corrections are calculated for the different production mechanisms. The values of the cross sections used by the experiments for $m_H = 125$ GeV are also given.

Figure 3 shows the branching ratios of the SM Higgs boson to different decay products. Branching ratios in Fig. 3 are given as a function of the Higgs boson mass. The plot on the left in Fig. 3 display the branching ratios in the range $90 < m_H < 200$ GeV, the region of particular interest, given the electro-weak fits. The final states most suitable for discovery at the LHC vary depending on the branching ratios, which are a function of the Higgs boson mass, and the relevant backgrounds. For $m_H < 2m_W$ the dominant decay mode is through $b\bar{b}$ with $B_b = 0.577^{+3.2\%}_{-3.3\%}$ for $m_H = 125$ GeV. The $\gamma\gamma$ final state has a small branching fraction, $(2.28 \times 10^{-3})^{+5.0\%}_{-4.8\%}$ for $m_H = 125$ GeV, but excellent γ/jet separation and γ energy resolution help to make this a very significant channel. The $H \to \tau\tau$ decay is accessible if the Higgs boson is produced in association with jets. Table 2 displays branching fractions of the SM Higgs boson with $m_H = 125$ GeV into different decays.

If the Higgs boson mass is large enough to make the WW and ZZ modes kinematically accessible, the $H \to WW^{(*)}$ final-states are powerful over a very large mass range (WW accounts for ∼95% of the branching fraction at $m_H \sim 160$ GeV), as is the $H \to ZZ^{(*)} \to 4\ell$ final state– the latter of which is commonly referred to as the "Golden Mode" as with four leptons in the final state the signal is easy to trigger on and allows for full reconstruction of the Higgs boson mass. For SM Higgs boson masses close to $2m_{top}$, the channel $H \to t\bar{t}$ opens up (see the right plot in Fig. 3), thus reducing the branching fraction of $H \to ZZ, WW$. Due to the very large cross section for the production of non-resonant $t\bar{t}$ pairs, the inclusive search for the SM Higgs boson with $H \to t\bar{t}$ is not considered feasible.

3. Results

In this section the results of the combination of the expectation and observation of the discovery channels discussed above are summarized. Results are presented in terms of upper exclusion limits and p-values. This is performed for the individual discovery channels and/or their combination, when available.

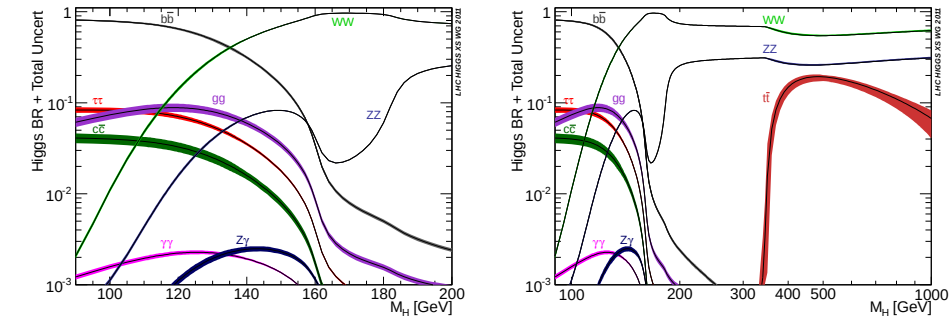

Figure 3. Branching fractions of the Standard Model Higgs boson to different decay products as a function of the mass (from Ref. [15]). The plot on the left and the right correspond to two different mass ranges.

Table 2. Branching ratios for the SM Higgs boson with $m_H = 125$ GeV (from Ref [15]). The errors correspond to current level of theory uncertainties and are expressed in terms of fractional deviations in %. The total width is given in MeV.

B_b	B_τ	B_μ	B_c	B_g
$0.577^{+3.2\%}_{-3.3\%}$	$0.0632^{+5.7\%}_{-5.7\%}$	$(2.2\times10^{-4})^{+6.0\%}_{-5.9\%}$	$0.0291^{+12.2\%}_{-12.2\%}$	$0.0857^{+10.2\%}_{-10.0\%}$
B_γ	$B_{Z\gamma}$	B_W	B_Z	Γ_H[MeV]
$(2.28\times10^{-3})^{+5.0\%}_{-4.8\%}$	$(2.28\times10^{-3})^{+9.0\%}_{-8.8\%}$	$^{+4.3\%}_{-4.2\%}$	$2.64^{+4.3\%}_{-4.2\%}$	$4.07^{+4.0\%}_{-3.9\%}$

Figure 4 shows the combination results presented by the CMS collaboration. The upper left plot corresponds to the exclusion limits in terms of the CL_s values in the mass range $110 < m_H < 145$ GeV. The dashed line shows the median of the background-only expectation while the green and yellow bands correspond to the 68% and 95% CL bands, respectively. The solid curve shows the experimentally observed upper exclusion limit. As a result of the strong excess observed in the data the observed exclusion limit for $m_H \approx 125$ GeV lies significantly above the median and outside the 95% CL bands. The regions where $CL_s < \alpha$ are excluded with at least $(1-\alpha)$ CL. The horizontal lines correspond to the 95% and 99% and 99.9% CL values. The upper right plot shows the expected p-values for a SM Higgs boson signal in the mass range and decay modes specified above and their combination. For $m_H \approx 125$ GeV CMS reports the $H \to ZZ^{(*)} \to 4\ell$ channel to be the most sensitive, closely followed by the di-photon search. The expected p-value for $m_H \approx 125$ GeV falls below the $5\,\sigma$ mark. CMS reports an observed local p-value at the $5\,\sigma$ level with an expected p-value of $5.8\,\sigma$ for $m_H = 125$ GeV. The global observed p-value is $4.5-4.6\,\sigma$, depending on the mass range considered for the evaluation of the trials factor. The lower right plot shows the compatibility of the location of the excess in the $\sqrt{s} = 7$ TeV and $\sqrt{s} = 8$ TeV data samples.

Figure 5 displays the combination results presented by the ATLAS collaboration. The upper plots correspond to CL_s in the entire range of the search, $110 < m_H < 600$ GeV. The solid and dashed lines correspond to the observed and expected CL_s. Dashed horizontal lines indicate the 95% and 99% CL values. Similar discussion as in the case of CMS results for $m_H \approx 125$ GeV apply here. It is worth noting that no significant excess is seen for m_H hypotheses outside the $m_H \approx 125$ GeV region. This translates into exclusions on the existence of another neutral Higgs boson with SM couplings with at least 95% and 99% in a wide range of masses. These results are expressed in terms of 95% CL upper limit exclusions on the signal strength in the

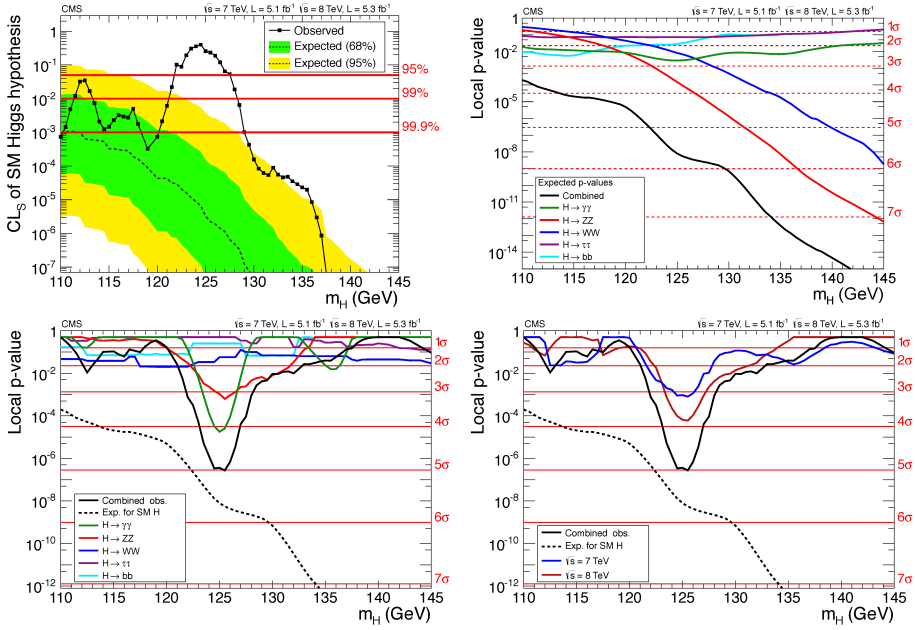

Figure 4. Results of the statistical combination of the various searches for the Higgs boson by the CMS experiment as a function of the m_H (from Ref. [10]). The upper left plot shows the combined CL_s for the SM Higgs boson hypothesis. The upper right and the lower left plots display the expected and observed local p-values of the individual search channels and their combination, respectively The lower right plot exhibits the observed local p-values for the $\sqrt{s} = 7$ TeV and $\sqrt{s} = 8$ TeV data sets separately. See text for more details.

upper right plot. The solid and dashed lines correspond to the observed and the median of the background-only expectation, respectively. The green and yellow bands correspond to the 65% and 95% CL bands, respectively. The solid and dashed lines in the lower left plot shows the combined observed and expected local p-values in a range $110 < m_H < 150$ GeV, respectively. The blue band corresponds to the 68% CL band. ATLAS reports an excess of $5.9\,\sigma$ with an expected local p-value of $4.9\,\sigma$ for $m_H = 126.5$ GeV. The global p-value becomes $5.3\,\sigma$ when considering the range $110 < m_H < 150$ GeV. The lower right plot shows the breakdown of the contribution from each individual channel. The dashed and solid lines correspond to the expected and observed p-values. In the region of the excess the most sensitive channel is the $H \to ZZ^{(*)} \to 4\ell$ decay closely followed by the $H \to WW^{(*)} \to \ell\nu\ell\nu$ and $H \to \gamma\gamma$ channels.

In summary, both the ATLAS and CMS collaborations independently observe a strong excess of the order of $5\,\sigma$ or more in a similar mass range around 125 GeV. The existence of additional bosons with SM couplings to other known particles is excluded with at least a 95% CL in the range $110 < m_H < 600$ GeV barring a narrow region around $m_H \approx 125$ GeV by both collaborations independently. Preliminary analyses on data samples collected during the second half of 2012 at $\sqrt{s} = 8$ TeV report the persistence of excess of events in the data in the range of $m_H \approx 125$ GeV consistent with that reported in Refs. [9, 10].

4. Conclusions

At present, all the data obtained from the many experiments in particle physics are in agreement with the Standard Model. In the Standard Model, there is one particle, the Higgs boson, that is responsible for giving masses to all the elementary particles. The ATLAS and CMS experiments

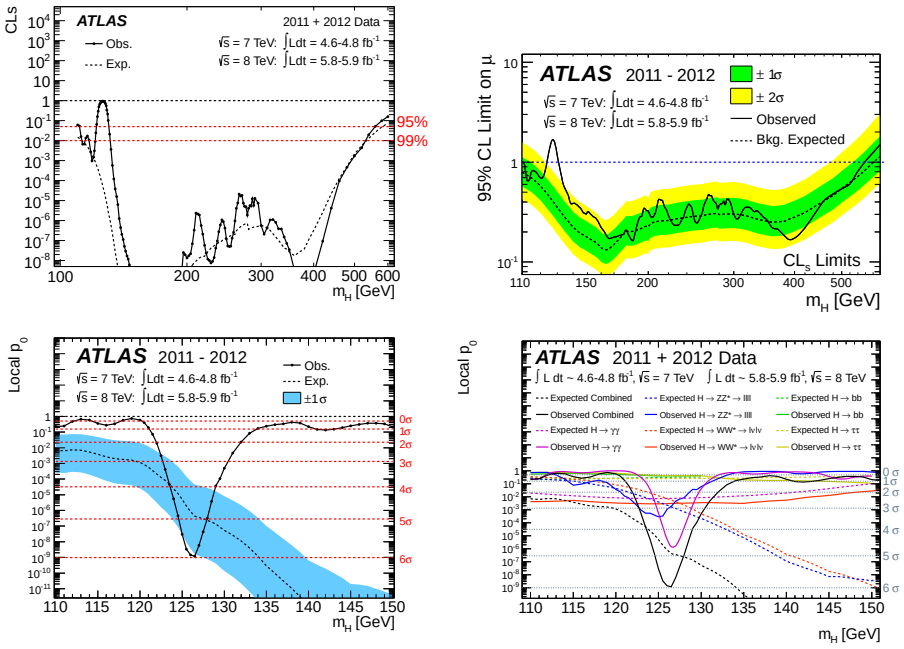

Figure 5. Results of the statistical combination of the various searches for the Higgs boson by the ATLAS experiment as a function of m_H (from Ref. [9]). The upper left and right plots plot display the CL_s for the SM Higgs boson hypothesis and 95% CL upper limit exclusion on the signal strength in the entire range of the SM Higgs boson search, respectively. The lower left plot shows the combined expected and observed the local p-values. The lower right plot displays the breakdown of the expected and observed p-values for the different channels. See text for more details.

at the Large Hadron Collider have declared the discovery of a Higgs boson with a mass around 125 GeV, as the result of the combination of several decay channels.

References

[1] S. Glashow, *Nucl.Phys.* **22**, 579 (1961).
[2] S. Weinberg, *Phys.Rev.Lett.* **19**, 1264 (1967).
[3] A. Salam, Proceedings to the eigth nobel symposium, may 1968, ed: N. svartholm (wiley, 1968) 357.
[4] S. Glashow, J. Iliopoulos and L. Maiani, *Phys.Rev.* **D2**, 1285 (1970).
[5] F. Englert and R. Brout, *Phys.Rev.Lett.* **13**, 321 (1964).
[6] P. W. Higgs, *Phys.Lett.* **12**, 132 (1964).
[7] P. W. Higgs, *Phys.Rev.Lett.* **13**, 508 (1964).
[8] G. Guralnik, C. Hagen and T. Kibble, *Phys.Rev.Lett.* **13**, 585 (1964).
[9] ATLAS Collaboration Collaboration (G. Aad *et al.*), *Phys.Lett.* **B716**, 1 (2012).
[10] CMS Collaboration Collaboration (S. Chatrchyan *et al.*), *Phys.Lett.* **B716**, 30 (2012).
[11] CDF Collaboration, D0 Collaboration Collaboration (T. Aaltonen *et al.*), *Phys.Rev.Lett.* **109**, 071804 (2012).
[12] J. C. Collins and D. E. Soper, *Ann.Rev.Nucl.Part.Sci.* **37**, 383 (1987).
[13] J. M. Campbell, J. Huston and W. Stirling, *Rept.Prog.Phys.* **70**, 89 (2007).
[14] LHC Higgs Cross Section Working Group, S. Dittmaier, C. Mariotti, G. Passarino and R. Tanaka (Eds.), *CERN-2011-002* (CERN, Geneva, 2011).
[15] LHC Higgs Cross Section Working Group, S. Dittmaier, C. Mariotti, G. Passarino and R. Tanaka (Eds.), *CERN-2012-002* (CERN, Geneva, 2012).